

NanoXerography: The Use of Electrostatic Forces to Pattern Nanoparticles

Michael G. Steward, Chad R. Barry, Stephen A. Campbell, Heiko O. Jacobs*

*Department of Electrical and Computer Engineering, University of Minnesota,
200 Union Street SE, Minneapolis, Minnesota 55455,*

**corresponding author, [hjacob@ece.umn.edu](mailto:hjacobs@ece.umn.edu).*

Abstract. Nanoparticles are considered as potential building blocks to fabricate future devices. This article reports on a new method to direct the assembly of nanoparticles onto surfaces. This method involves generating charge patterns with 100 nm resolution. To fabricate these charge patterns a new process has been developed. In this process a flexible conductive electrode is brought into contact with a 80-nanometer thick electret film supported by a silicon chip. Charge patterns in the electret film were generated by applying a voltage pulse between the electrode and silicon chip. Areas as large as 1 square centimeter were patterned with charge at a resolution better than 150 nanometers in 10 seconds. These high resolution charge patterns attract nanoparticles. First results on the electrostatically directed assembly of nanoparticles from a powder, gas phase (aerosol), and liquid phase (suspension) are reported. The accomplished resolution is 400 nanometers and more than two orders of magnitude greater than that achieved by today's xerographic printers.

Introduction. Nanoparticles are considered as the building blocks of future nanotechnological devices. Multidimensional assembly of nanoparticles will enable the fabrication of many profound devices such as single electron transistors¹⁻³, quantum-effect-based lasers^{4,5}, photonic band gap materials, filters, wave-guides⁶⁻⁸, and high-density data storage⁹⁻¹¹. The use of nanoparticles as building blocks, however, requires novel assembling strategies. Most actively studied approaches include: (i) single particle manipulation^{2,12-16}, (ii) random particle deposition^{13,17-19}, and (iii) parallel particle assembly-based on self-assembly^{7,20-24}.

Single particle manipulation and random particle deposition are useful to fabricate and explore new device architectures. However, inherent disadvantages such as the lag in yield and speed will be difficult to overcome in the future. Fabrication strategies that rely on mechanisms of self-assembly^{6,8,25} may prevail these difficulties. Self-assembly is well known in chemistry and biology.

Self-assembly can handle extremely small objects and is massively parallel. The self-assembly occurs due to forces between the objects themselves. We and others have begun to use self-assembly to assemble nanoparticles onto substrates. Most actively investigated areas, currently, use protein recognition²⁶⁻²⁹, DNA hybridization^{22,23,30,31}, hydrophobicity / hydrophilicity^{32,33}, and magnetic interactions^{10,11,24}.

In our own research in this area, we focus on electrostatic interaction because it is long-range and non-material specific (any particle can be trapped).³⁴ The most established example of patterning particles with electrostatic forces is Xerography. Images are formed in Xerography by capturing small pigment particles with a charge pattern on an appropriate carrier (electret). The lateral resolution achieved in Xerography is about 100 μm .³⁵⁻³⁸

In 1988 Stern *et al.* demonstrated that a modified atomic force microscope can be used to generate and image charge patterns with ~ 150 nm resolution.³⁹ Since then most of the work including our own focused on using trapped charges for high-density data storage.⁴⁰⁻⁴² In 1998 Wright and Chetwynd suggested that such high-resolution charge patterns could be used as templates for self-assembly and as nucleation sites for molecules and small particles.⁴³ This type of “Nanoxerography” has not been realized because the fabrication of charge patterns over large areas has been time consuming. The fastest scanning probe system requires 1.5 days to pattern an area of 1 cm^2 .⁴² To overcome this problem we recently developed a parallel printing process to pattern charges with ~ 100 nm resolution.³⁴ In this printing process a conductive, flexible electrode is used in place of a single point contact to inject and trap charges over areas of 1 cm^2 in ~ 10 seconds. The flexible micro-patterned electrode is designed to form multiple electric contacts of different size and shape to a rigid surface to expose the entire surface in a single step. This patterning approach opens up the route to nanoxerography since it allows the fabrication of charge patterns over large areas in large quantities. Many chips carrying high resolution charge patterns can be fabricated within an hour, which enables us to study the assembly of different species, inorganic particles, or organic molecules onto charged areas in a reasonable amount of time. In this study we report on recent improvements in the printing apparatus and demonstrate the use of trapped charge to pattern inorganic nanoparticles from a powder, gas phase (aerosol), and liquid phase (suspension).

Materials and Methods. The charge patterning process is illustrated in Figure 1. A silicon chip coated with a thin film electret was placed on top of a flexible conductive electrode. The electret on the silicon chip was Poly(methylmethacrylate) (PMMA, an 80-nm film, on a silicon wafer); PMMA

is commercially available, and has good charge storage capabilities.⁴⁴ We used a 2% solution of 950 K PMMA in chlorobenzene (MicroChem Co.) and spin coating at 5000 rpm to form the electret film on the wafer. The wafers were $\langle 100 \rangle$ n-doped silicon with a resistivity of 3 ohm cm that we cleaned in 1% solution of Hydrofluoric acid to remove the native oxide prior to spin coating. The spin coated wafers

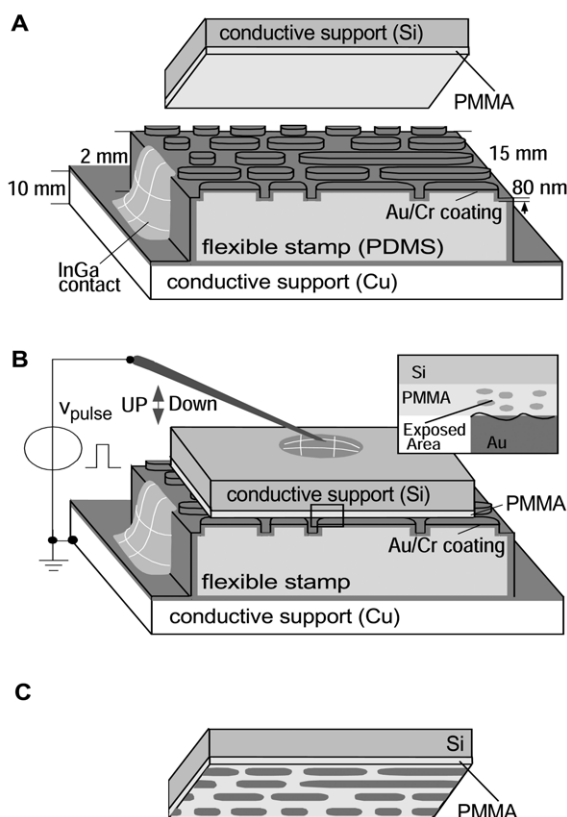


Figure 1. Principle of parallel charge patterning. (A) A thin film of PMMA supported on a doped, electrically conducting Si chip is placed on top of a flexible, gold coated stamp that is supported on a copper plate. (B) A needle, attached to a micromanipulator and connected to an electrometer is brought into contact with the silicon chip. An external voltage is applied between the needle and the copper support to generate a pattern of charge in the PMMA. (C) The silicon chip is removed with the PMMA carrying a charge pattern.

were then baked at $90 \text{ }^\circ\text{C}$ for 1 hour under vacuum before being cut into 1 cm^2 squares. To

contact the chips electrically we spread liquid InGa onto the back side of the chip. The chips were then placed on top of the flexible conductive electrode.

The flexible conductive electrode was formed using a 5 mm thick poly(dimethylsiloxane) (PDMS) stamp, patterned in bas relief as previously described⁴⁵. The patterned surface of the PDMS stamp was made electrically conducting by thermal evaporation of 80 nm of gold onto it. To obtain low resistance electrical connections to the electrode surface, InGa (a liquid metal alloy, Aldrich) was applied to the side walls of the electrode and at the interface between the electrode and the copper plate.

A metallic needle attached to a micromanipulator is used to form a low resistance contact with the InGa on the back of the chip. A potential of approximately 10-30V is applied between the needle and the copper plate to get an exposure current of 1-10mA/cm². After 1-10 seconds of exposure, the chip containing a trapped charge pattern is removed. After removal, the charge pattern is characterized using Kelvin Probe Force Microscopy (KFM).⁴⁶ KFM involves the use of an Atomic Force Microscope (AFM) probe to detect electrostatic forces. In previous research we developed a KFM procedure that enables us to measure the charge and surface potential distribution with 100 nm scale resolution.⁴⁶⁻⁴⁹

To assemble nanoparticles onto charged areas, we investigated three different procedures (Fig. 2). In all experiments we used commercially available carbon toner, red iron oxide particles, and graphitized carbon particles.⁵⁰ In the first procedure, we dipped PMMA-coated chips carrying a charged pattern into dry powders of nanoparticles and removed the loosely held material in a stream of dry nitrogen. In the second procedure, we exposed chips carrying a charge pattern to a cloud of nanoparticles. The particle cloud was formed inside a cylindrical glass chamber (10 cm in diameter and 5 cm high) using a fan to mix the nanoparticles with the

surrounding gas (Air or Nitrogen). A laser pointer was used to visualize (due to scattering of light) the suspended nanoparticles in the chamber. This particular experiment was used to test whether nanoparticles can be assembled onto charged areas directly from the gas phase. In the third procedure, we used a liquid suspension of nanoparticles. To suspend the nanoparticles we used non-polar liquids such as Perfluorodecalin (#601, Sigma-Aldrich, USA) and FLUORINERT (FC-77, 3M). These fluorinated solvents have a low relative dielectric constant of ~1.8 to provide maximum electrostatic interaction. To agitate the nanoparticles, we used an ultrasonic bath

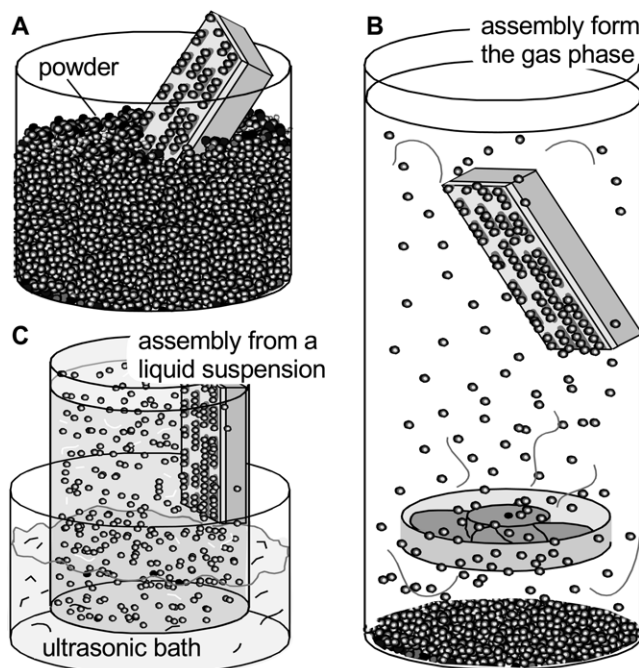


Figure 2. Illustrations of three different assembly principles. (A) The charged chip is immersed into nanoparticle powder. (B) The charged chip is exposed to nanoparticles that are suspended in the gas phase. (C) The silicon chip is immersed into a solution that contains nanoparticles that are agitated using an ultrasonic bath.

(Branson 3510, DanBury, CT). The chip containing a charge pattern is placed into the

agitated suspension of nanoparticles for 10-20 seconds. To remove any loosely held particles the chip is transferred into a vial containing the solvent without nanoparticles and sonicated for another 10-20 s. Finally it is dried with a stream of dry nitrogen. We noticed that the nanoparticles tend to agglomerate in non polar solvents. Agitation of the suspension with an ultrasonic bath allows us to minimize this effect. Nevertheless, we find that agglomerates can become as large as 400 nm and limit the resolution.

Results. Representative patterns of localized charge recorded by KFM are illustrated in Figure 3. Figure (A) shows the surface potential for a surface patterned in a way that simulates high-density data storage. The bits (full-width at half-maximum, FWHM, <150 nm, density = 5 Gbits/cm²) are randomly distributed. To write this charge pattern, we exposed the PMMA film with a current density of 20 mA/cm² for 10 seconds with the metal-coated stamp positive. Figures (B) and (C) show 1 μm-sized charged dots and 200 nm (FWHM) wide parallel lines that were written with a current density of 13 mA/cm² for 10 seconds and 30 mA/cm² for 2 seconds. The illustrated patterns are representative of those observed over large areas. For the sample illustrated in (C) we have noticed variations in the detected surface potential difference across the surface of the chip. The origin of the variations has not yet been characterized. With clean surfaces and new stamps we are typically able to pattern charge over areas of 1 cm². The smallest charge patterns we have generated are about 150 nm in size. At these scales, the transfer function of the Kelvin probe limits the resolution and the patterns are not well resolved.⁴⁸ It is important to notice that the amplitudes of the detected potential difference between charged areas and uncharged areas for different samples can not be compared directly. The recorded amplitude depends on the exposure conditions, the size and shape of the charged areas,

the condition of the AFM tips, and the sensitivity of the Kelvin probe.

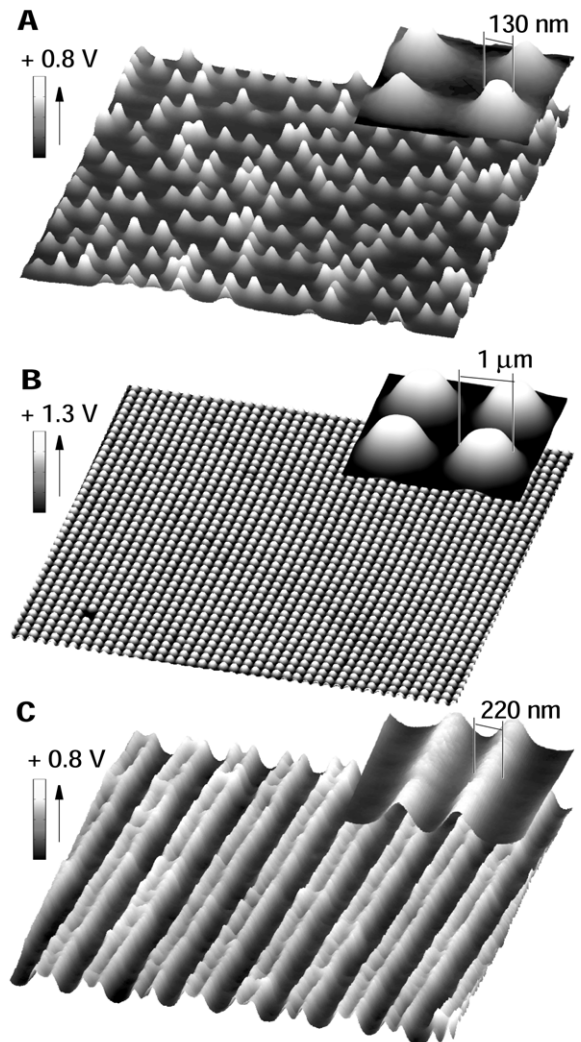
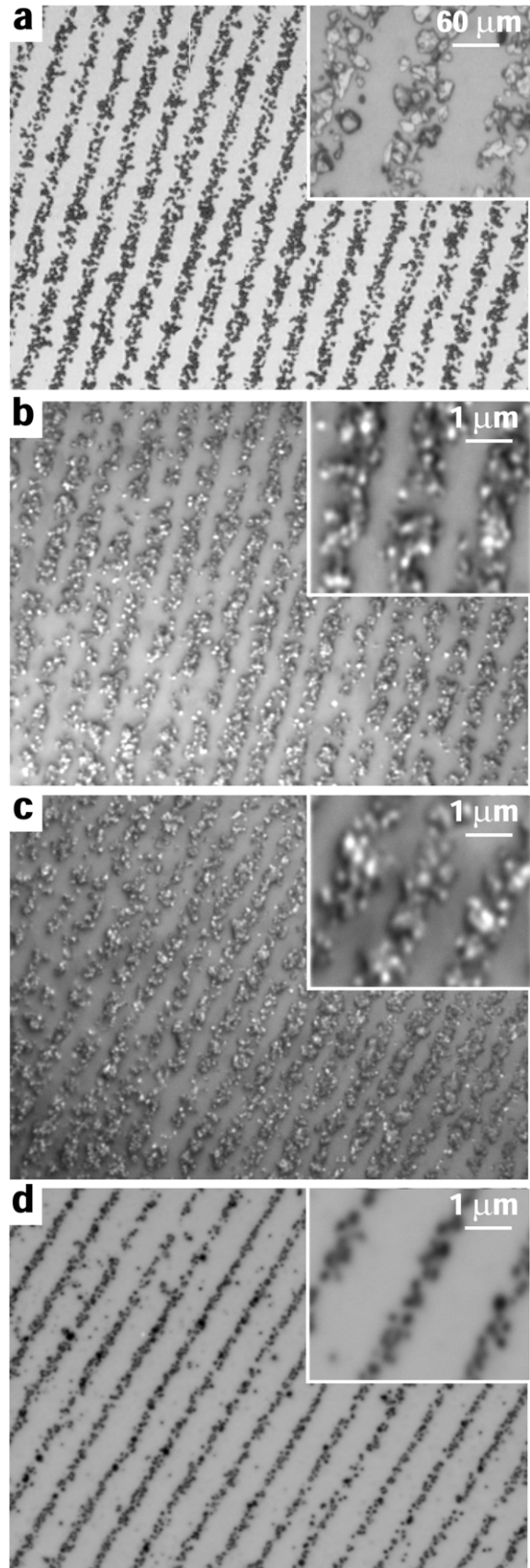


Figure 3. Kelvin probe force microscopy images of patterns of positive charge. (A) Surface potential distribution of a test pattern of high density data storage with <150 nm sized bits (FWHM). The pattern was generated using a stamp carrying 150 nm wide circular posts that were 90 nm high. (B) Surface potential images of positively charged dots 1 μm in diameter that were generated using circular posts that were 1.4 μm high. (C) Surface potential image of 220 nm (FWHM) positively charged parallel lines generated using a stamp carrying 1 μm wide parallel lines that were 900 nm wide and that were slightly higher at the edge than in the center.

Figure 4 shows representative images of charged based printing using particles from a powder, gas, and liquid phase. The images show patterns of carbon toner ($\sim 25 \mu\text{m}$), red iron oxide ($< 500 \text{ nm}$), and graphitized carbon ($\sim 80 \text{ nm}$) that are trapped at charged areas on PMMA. The resolution achieved was $\sim 60 \mu\text{m}$ for Xerox toner from a powder, $\sim 1 \mu\text{m}$ for red iron oxide particles from a powder, $\sim 1 \mu\text{m}$ for red iron oxide particles from the gas phase, and $\sim 800 \text{ nm}$ for graphitized carbon from a suspension in Perfluorodecalin. We have not yet determined the actual charge on these particles. In the presented results the different particles were trapped with positive charge patterns. However, we found that the same particles can be trapped with negative charge patterns as well. This phenomenon suggests that the assembly process is dominated by a real charge – induced dipole interaction; i.e. trapped charge in the thin film electret induce a dipole on the particle causing an attractive net force between a polarizable particle and a charged surface area. It is quite remarkable that the trapped charges in the 80 nm thin PMMA film exhibit a sufficient electrostatic force to direct the assembly of the almost 3 orders of magnitude larger toner particles using the powder method.

Figure 5 shows an SEM image of graphitized carbon nanoparticles that were assembled onto 400 nm wide positively charged lines. The accomplished resolution is more than 2 orders of magnitude higher than what is achieved in xerographic printing. Figure 5b compares this SEM image with an SEM image of a typical Xerox toner particle.

Figure 4. Optical microscope images of different particles that were assembled from a powder, liquid, and gas phase. (A) $60 \mu\text{m}$ wide parallel lines of toner particles, $\sim 25 \mu\text{m}$ in size, assembled from a powder. (B) $1 \mu\text{m}$ wide parallel lines of red iron oxide particles, $< 500 \text{ nm}$ in size, assembled from a powder. (C) $1 \mu\text{m}$ wide parallel lines of red iron oxide particles, $< 500 \text{ nm}$ in size, assembled from the gas phase. (D) 800 nm wide parallel lines of graphitized carbon particles, $< 100 \text{ nm}$ in size, assembled from a liquid phase. In this demonstration, all particles were trapped with positive charge. It was also possible to trap nanoparticles at negative charge patterns.



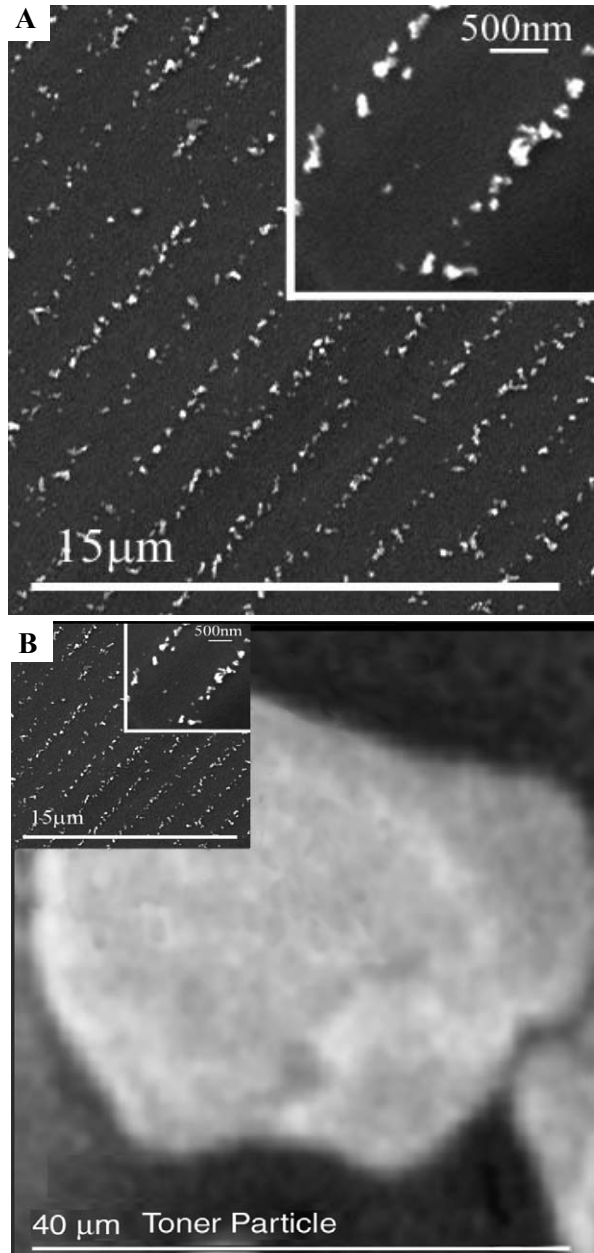


Figure 5. SEM images of graphitized carbon nanoparticles and a Xerox toner particle. (A) 400 nm wide parallel lines of graphitized carbon particles assembled from a liquid phase. (B) Same image overlaid onto an image of a typical 40 μm sized toner particle.

Conclusion. We demonstrated the directed parallel self-assembly of nanoparticles onto charged surface areas with sub-micrometer resolution. We developed a strategy for patterning charge in electrets that extends previous serial techniques⁴⁰⁻⁴² and is currently the only parallel method available

with ~100 nm resolution. Many questions concerning this process have yet to be answered. We do not understand the nature of the contact on a molecular length scale, for example we do not know if a true van der Waals contact is established or not. However, this "new type of contact" allows us to fabricate charge based receptors to direct the assembly of particles with dimensions ranging from 20 nm – 30 μm. The resolution demonstrated in this report is 400 nm and limited by the coexistence of larger agglomerated particles.

Since charge patterns with ~100 nm resolution can be generated by our parallel process, higher resolution assembly is perceived to be possible. Even at a 10 nm length scale electrostatic forces are estimated to be one order of magnitude larger than the disordering force due to brownian motion. A number of fundamental studies is required, however, to determine the best experimental conditions to accomplish the ultimate resolution of Nanoxerographic printing. We expect the process to be dependant upon the actual charge, electric polarizability, and thermal energy of the particle, the electric field strength at the substrate surface, the particle–surface interaction, the suspending medium, and the pressure.

- ¹ M. H. Devoret and R. J. Schoelkopf, *Nature* **406**, 1039-1046 (2000).
- ² T. Junno, M. H. Magnusson, S. B. Carlsson, K. Deppert, J. O. Malm, L. Montelius, and L. Samuelson, *Microelectronic Engineering* **47**, 179-183 (1999).
- ³ R. J. Schoelkopf, P. Wahlgren, A. A. Kozhevnikov, P. Delsing, and D. E. Prober, *Science* **280**, 1238-1242 (1998).
- ⁴ S. Fafard, K. Hinzer, S. Raymond, M. Dion, J. McCaffrey, Y. Feng, and S. Charbonneau, *Science* **274**, 1350-1353 (1996).
- ⁵ J. Faist, F. Capasso, D. L. Sivco, C. Sirtori, A. L. Hutchinson, and A. Y. Cho, *Science* **264**, 553-556 (1994).
- ⁶ Y. N. Xia, B. Gates, and Z. Y. Li, *Advanced Materials* **13**, 409-413 (2001).

- ⁷ T. S. Phely-Bobin, R. J. Muisener, J. T. Koberstein, and F. Papadimitrakopoulos, *Advanced Materials* **12**, 1257-+ (2000).
- ⁸ D. J. Norris and Y. A. Vlasov, *Advanced Materials* **13**, 371-376 (2001).
- ⁹ H. Brune, M. Giovannini, K. Bromann, and K. Kern, *Nature* **394**, 451-453 (1998).
- ¹⁰ C. Petit, A. Taleb, and M. P. Pileni, *Advanced Materials* **10**, 259 ff. (1998).
- ¹¹ W. L. Zhou, E. E. Carpenter, J. Lin, A. Kumbhar, J. Sims, and C. J. O'Connor, *European Physical Journal D* **16**, 289-292 (2001).
- ¹² C. Baur, A. Bugacov, B. E. Koel, A. Madhukar, N. Montoya, T. R. Ramachandran, A. A. G. Requicha, R. Resch, and P. Will, *Nanotechnology* **9**, 360-364 (1998).
- ¹³ L. T. Hansen, A. Kuhle, A. H. Sorensen, J. Bohr, and P. E. Lindelof, *Nanotechnology* **9**, 337-342 (1998).
- ¹⁴ T. J. Krinke, H. Fissan, K. Deppert, M. H. Magnusson, and L. Samuelson, *Applied Physics Letters* **78**, 3708-3710 (2001).
- ¹⁵ R. Resch, A. Bugacov, C. Baur, B. E. Koel, A. Madhukar, A. A. G. Requicha, and P. Will, *Applied Physics* **67**, 265-271 (1998).
- ¹⁶ M. Sitti and H. Hashimoto, *Ieee/Asme Transactions on Mechatronics* **5**, 199-211 (2000).
- ¹⁷ K. Matsumoto, Y. Gotoh, T. Maeda, J. A. Dagata, and J. S. Harris, *Japanese Journal of Applied Physics Part* **38**, 477-479 (1999).
- ¹⁸ L. Montelius, T. Junno, S. B. Carlsson, and L. Samuelson, *Microelectronic Engineering* **35**, 281-284 (1997).
- ¹⁹ L. Montelius, T. Junno, S. B. Carlsson, M. H. Magnusson, K. Deppert, H. Xu, and L. Samuelson, *Microelectronics & Reliability* **38**, 943-950 (1998).
- ²⁰ D. I. Gittins, D. Bethell, D. J. Schiffrin, and R. J. Nichols, *Nature* **408**, 67-69 (2000).
- ²¹ W. A. Lopes and H. M. Jaeger, *Nature* **414**, 735-738 (2001).
- ²² C. M. Niemeyer, *Applied Physics a* **68**, 119-124 (1999).
- ²³ C. M. Niemeyer, B. Ceyhan, S. Gao, L. Chi, S. Peschel, and U. Simon, *Colloid & Polymer Science* **279**, 68-72 (2001).
- ²⁴ Y. Saado, T. Ji, M. Golosovsky, D. Davidov, Y. Avni, and A. Frenkel, *Optical Materials* **17**, 1-6 (2001).
- ²⁵ J. H. Fendler, *Chemistry of Materials* **13**, 3196-3210 (2001).
- ²⁶ C. Chothia and J. Janin, *Nature* **256**, 705-8 (1975).
- ²⁷ J. Janin, *Progress in Biophysics & Molecular Biology* **64**, 2-3 (1995).
- ²⁸ J. T. Moore, P. D. Beale, T. A. Winningham, and K. Douglas, *Applied Physics Letters* **71**, 1264-6 (1997).
- ²⁹ M. J. Dabrowski, J. P. Chen, H. Q. Shi, W. C. Chin, and W. M. Atkins, *Chemistry & Biology* **5**, 689-697 (1998).
- ³⁰ E. Braun, Y. Eichen, U. Sivan, and G. Benyoseph, *Nature* **391**, 775-778 (1998).
- ³¹ P. Malherbe, J. G. Richards, H. Gaillard, A. Thompson, C. Diener, A. Schuler, and G. Huber, *Molecular Brain Research* **71**, 159-170 (1999).
- ³² I. S. Choi, N. Bowden, and G. M. Whitesides, *Angewandte Chemie. International Ed. in English* **38**, 3078-3081 (1999).
- ³³ P. D. Yang, A. H. Rizvi, B. Messer, B. F. Chmelka, G. M. Whitesides, and G. D. Stucky, *Advanced Materials* **13**, 427-431 (2001).
- ³⁴ H. O. Jacobs and G. M. Whitesides, *Science* **291**, 1763-1766 (2001).
- ³⁵ D. M. Pai and B. E. Springett, *Reviews of Modern Physics* **65**, 163-211 (1993).
- ³⁶ R. Groff, P. Khargonekar, D. Koditschek, T. Thieret, and L. K. Mestha, *Proceedings of the 38th IEEE Conference on Decision and Control* **2** (1999).
- ³⁷ K. Takiguchi, *Proceedings of 5th International Conference on High Technology: Imaging Science and Technology, Evolution and Promise. World Techno Fair in Chiba '96. Chiba Univ* (1996).
- ³⁸ S. W. Ing, *IEEE Trans. on Electron Devices* **36** (1989).
- ³⁹ J. E. Stern, B. D. Terris, H. J. Mamin, and D. Rugar, *Applied Physics Letters* **53**, 2717-19 (1988).
- ⁴⁰ R. C. Barrett and C. F. Quate, *Ultramicroscopy* **42-44**, 262 (1992).
- ⁴¹ J. E. Stern, B. D. Terris, H. J. Mamin, and D. Rugar, *SPIE* **1855**, 194 (1993).
- ⁴² A. Born and R. Wiesendanger, *Applied Physics a* **68**, 131-135 (1999).
- ⁴³ W. M. D. Wright and D. G. Chetwynd, *Nanotechnology* **9**, 133-142 (1998).
- ⁴⁴ H. S. Nalwa, *Ferroelectric Polymers. Chemistry, Physics and Applications* (New York, Marcel Dekker, 1995); K. Mazur, *J. Phys.* **D30**, 1383 (1997).
- ⁴⁵ Y. N. Xia and G. M. Whitesides, *Annual Review of Materials Science* **28**, 153-184 (1998).
- ⁴⁶ H. O. Jacobs, H. F. Knapp, S. Muller, and A. Stemmer, *Ultramicroscopy* **69**, 39-49 (1997).
- ⁴⁷ H. O. Jacobs, H. F. Knapp, and A. Stemmer, *Review of Scientific Instruments* **70**, 1756-1760 (1999).
- ⁴⁸ H. O. Jacobs, P. Leuchtman, O. J. Homan, and A. Stemmer, *Journal of Applied Physics* **84**, 1168-1173 (1998).
- ⁴⁹ H. O. Jacobs and A. Stemmer, *Surface & Interface Analysis* **27**, 361-367 (1999).
- ⁵⁰ The black toner (product number 13R55) was obtained from Xerox Co., the red iron oxide and graphitized carbon was obtained from PolyScience, Niles, Illinois.